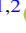CrossMark

Composition and Sticking of Hot Chondritic Dust in a Protoplanetary Hydrogen Atmosphere

Cynthia Pillich[1,2] , Tabea Bogdan[2] , Janosch Tasto[1,2] , Joachim Landers[1,2] , Gerhard Wurm[2] , and Heiko Wende[1,2]
[1] University of Duisburg-Essen and Center for Nanointegration Duisburg-Essen (CENIDE), Faculty of Physics, Lotharstr. 1, D-47057 Duisburg, Germany
[2] University of Duisburg-Essen, Faculty of Physics, Lotharstr. 1, D-47057, Germany

Abstract

The sticking properties of dust in early phases of planet formation depend on the thermal history and ambient atmosphere. Therefore, dust will change its ability to build larger aggregates in collisions, depending on its location in protoplanetary disks. We aim at quantifying the change in sticking properties as chondritic dust is heated under various atmospheric conditions. In laboratory experiments, we milled two different meteorites (Sayh al Uhaymir 001 and Allende) to dust and formed millimeter-size cylinders. These cylindrical aggregates were sequentially heated from 600 to 1400 K in vacuum and in a hydrogen atmosphere, with compositional changes being tracked via Mössbauer spectroscopy. Using a Brazilian splitting test, the splitting tensile strength was determined. At higher temperatures, iron in silicates is reduced to metallic Fe(Ni) within the hydrogen atmosphere. In any case, adhesive forces are strongly increased by orders of magnitude from 1000 to 1400 K with minimum variations, depending on the atmospheric conditions. The dust in protoplanetary disks becomes ever more sticky, approaching a sublimation line upon exposure to temperatures of about 1400 K.

Unified Astronomy Thesaurus concepts: Protoplanetary disks (1300); Planet formation (1241)

1. Introduction

The sticking of dust in mutual collisions drives the early phases of planet formation. Therefore, sticking properties are of the utmost importance. The growth and evolution of grains in this initial period are frequently studied (Dominik & Tielens 1997; Youdin & Goodman 2005; Blum & Wurm 2008; Kataoka et al. 2013; Johansen et al. 2014; Yamamoto et al. 2014; Kimura et al. 2015; Musiolik et al. 2016; de Beule et al. 2017; Demirci et al. 2017, 2019; Gärtner et al. 2017; Gundlach et al. 2018; Musiolik & Wurm 2019; Bogdan et al. 2019; Steinpilz et al. 2019; Pinilla et al. 2021).

The location in the disk is an important factor to be considered. As the adhesive interaction depends on the surfaces of dust particles, all conditions that change the composition and therefore the surface might influence the sticking. The temperature might change in local or short events, i.e., during chondrule formation (Connolly & Jones 2016), in the context of large impacts (Leinhardt & Stewart 2012), or during stellar outbursts (Kley & Lin 1999), but the dust particles in the protoplanetary disk are also regularly considered to drift inward toward the star, where they are exposed to ever higher temperatures (Weidenschilling 1977).

Our earlier works suggest that there is a spatial region in a disk that favors planetesimal formation between 900 and 1300 K due to the local composition of the dust and a lower surface water fraction, which lead to the increased sticking of grains (Bogdan et al. 2020; Pillich et al. 2021). In this paper, we add to our former results and strengthen these theses of a sweet spot for planetesimal formation. Bogdan et al. (2020) and Pillich et al. (2021) used dust created by grinding a piece of the meteorite Sayh al Uhaymir 001 (SaU). It is classified as an L4/

5-type chondrite that has undergone a slight thermal metamorphosis, but, in general, its composition is close to the mineral mix that might be expected in protoplanetary disks. We note that the use of meteorites and their grinding is not meant to simulate the recycling of asteroids, e.g., their destruction and reaccumulation. The meteorites only serve as a reservoir of material with a composition that dust might have at moderate temperatures in the solar nebula or, more generally, protoplanetary disks.

Our work simulates early growth phases up to pebble size (millimeter to decimeter) in an inner protoplanetary disk, based on material drifting inward from cool temperatures to hot temperatures. If the sticking properties change with location, this changes the potential size of the dust aggregates and this might seed local planetesimal formation at high temperatures, maybe adding a bias to, e.g., Mercury-like planets.

Simulating the drift, we heated the dust at increasing temperatures in vacuum ranging from 600 K up to 1400 K. The surface energies were deduced based on tensile strength measurements and showed a considerable increase in sticking after heating at the highest temperatures by orders of magnitude. To see how sensitive these results are in terms of material composition and atmospheric conditions, we continue this work with two variations here.

1. We add another sample to the data set, i.e., using material from the Allende meteorite as a starting point. Classified as CV3, the Allende meteorite is unequilibrated and therefore even closer to a realistic mix of minerals in the protoplanetary disk.
2. As gaseous hydrogen is the most abundant element in protoplanetary disks, we additionally followed the same preparation and measurement procedure for both meteorites, including the SaU that we used previously, but tempered both in a low-pressure hydrogen atmosphere, to see how the presence of hydrogen might influence the tensile strength.

One first result of this study, somewhat related to adhesion but with a focus on magnetic properties, has already been reported in Bogdan et al. (2023). We showed that tempering Allende in the hydrogen atmosphere results in the formation of ferromagnetic iron–nickel constituents, which might be important in the context of magnetic aggregation and the formation of Mercury-like planets (Kruss & Wurm 2018, 2020). In the present study, we focus on the adhesive properties instead of magnetic agglomeration, though.

2. Relative Surface Energy

As in our earlier work, in Pillich et al. (2021) and Bogdan et al. (2020), we quantify the average adhesion by measurements of the splitting tensile strength for each heating temperature and sample. The basic method for this is the Brazilian splitting test, where a force is applied to the mantle of a cylinder until it breaks in half. The entire workflow, including preparation and measurement, corresponds to the super dry sample in Pillich et al. (2021). We refer to this work for details, but for readability we summarize the basic steps here.

The first step consists of milling the meteorite to micrometer dust in order to allow a mix of grains to be sticky enough to form stable aggregates. The dust is then pressed into millimeter-sized cylinders. These cylinders are heated for 1 hr at temperatures ranging from 600 to 1400 K. The heating takes place either in vacuum or in a hydrogen atmosphere, in which the heating chamber is continuously flushed with hydrogen, keeping a constant pressure of about 1 mbar during the entire heating process, close to realistic conditions in protoplanetary disks.

We note that the pressures in disks vary strongly, depending on the disk model and evolutionary time from millibar close in and early on to anything below far out (Hayashi et al. 1985; Wood 2000). Therefore, if taken one to one, our hydrogen pressure comes close to the region where we expect high temperatures. On the other side, vacuum conditions with about 10^{-2}–10^{-3} mbar would rather correspond to more moderate disk temperatures, e.g., at Earth distance in the Solar Nebula. The important point here, though, is that the pressure is low enough in the experiments to suppress the reoxidization of iron as seen in our earlier work.

After the sample cylinder is cooled down, it is broken by the Brazilian test and the force applied is translated into the tensile strength. Previous works use this technique and find power laws of the tensile strength dependence on the filling factor Φ (Meisner et al. 2012; Steinpilz et al. 2019; Bischoff et al. 2020; Bogdan et al. 2020). As described in more detail in our first two papers, Bogdan et al. (2020) and Pillich et al. (2021), we translate the tensile strength into an effective surface energy given by

$$\gamma_e = 1.3 \cdot d \cdot \frac{\sigma_0}{N_0 \Phi_0}. \tag{1}$$

Here, d is the grain size. As in our earlier works (Bogdan et al. 2020; Pillich et al. 2021), the size was measured for each sample with a Mastersizer 3000. Size always refers to the size of the dust grains, which make up the cylinder, i.e., the smallest units that still disperse easily. Up to 1100 K, the grain sizes do not vary significantly. At higher temperatures, the grain sizes systematically increase. This might be an indication that grains partially sinter together (Bogdan et al. 2019). The sizes slightly

vary for the different samples (SaU / Allende, vacuum / H_2), but are on the order of a few micrometers, initially increasing to tens of micrometers at the highest temperatures. Furthermore, σ_0 in Equation (1) is the average tensile strength at the average filling factor Φ_0 for the respective sample of cylinders tested. The filling factors are on the order of 0.4. The tensile strength varies the most by orders of magnitude toward higher temperatures up to values of a few 100 kPa. For the coordination number, we assume $N_0 = 3$. Keeping in mind that γ_e is only an effective surface energy, values at low temperatures are on the order of $\gamma_e \sim 0.1$–$1\,Jm^{-2}$ (Bogdan et al. 2020; Pillich et al. 2021). To allow a base material independent comparison, we define a relative surface energy for the different samples. To do so, we relate all values of a data set to one reference value, for which we chose 600 K here. We then define the relative surface energy as $\gamma_e/\gamma_e(600\,\mathrm{K})$. The relative surface energies for all four sample sets, i.e., the two different meteorites SaU and Allende, each heated under vacuum and in a hydrogen atmosphere, are shown in Figure 1.

It is striking that the measurements do not show a significant difference. In all four cases, the relative surface energy increases monotonously and rises by orders of magnitude between about 1000 and 1400 K. The Allende data fit the SaU data in this respect.

In our earlier work, in Pillich et al. (2021), we attributed the strong increase of the tensile strength at high temperatures to the complete loss of water. In this case, mostly silanol surfaces would determine the surface energy, if silicates are responsible as underlying dominant minerals (Kimura et al. 2015). If the minerals change, this compositional dependence might change. We found, e.g., that the material became more adhesive if the sample was tempered at moderate temperatures but in an oxidizing atmosphere. This led to an increased iron oxide fraction and an increase in the surface energy (Bogdan et al. 2020; Pillich et al. 2021). Avoiding oxidation by tempering SaU in vacuum, no iron oxide formed. The abundance of pyroxenes decreased, while the fraction of olivines increased (Pillich et al. 2021). The influence of these compositional changes on the tensile strength was rather subtle, though.

The question is whether a different compositional variation occurs, despite our results for the relative surface energy not hinting at any influence of the heating atmosphere. To track the composition, we carried out Mössbauer spectroscopy and synchrotron X-ray diffraction (XRD) experiments.

3. Synchrotron XRD

XRD data of the Allende meteorite were recorded at beamline ID22 of the European Synchrotron Radiation Facility in Grenoble, France. Following a measurement of the untreated powder sample at room temperature, the environmental temperature was raised with a rate of $2\,\mathrm{K\,min^{-1}}$ up to 1200 K. During this ramping, a diffractogram was measured every 2 minutes to observe dynamic processes induced by heating the sample. The capillary containing the Allende powder had been evacuated before mounting it inside the experimental setup. Therefore, the sample relates to the tensile strength measurements of Allende tempered under vacuum.

Due to being a natural sample with a broad mineralic distribution, all the diffractograms show a large number of diffraction peaks (see Figure 2), where most can be ascribed to
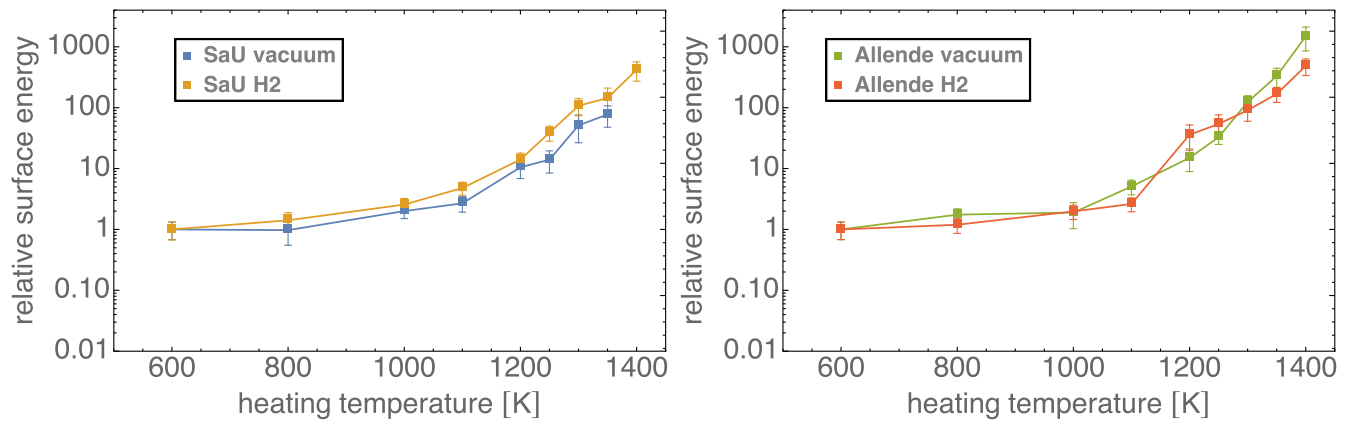
Figure 1. Relative surface energies over heating temperature for the two different samples, meteorites SaU and Allende, each being heated in vacuum and hydrogen.
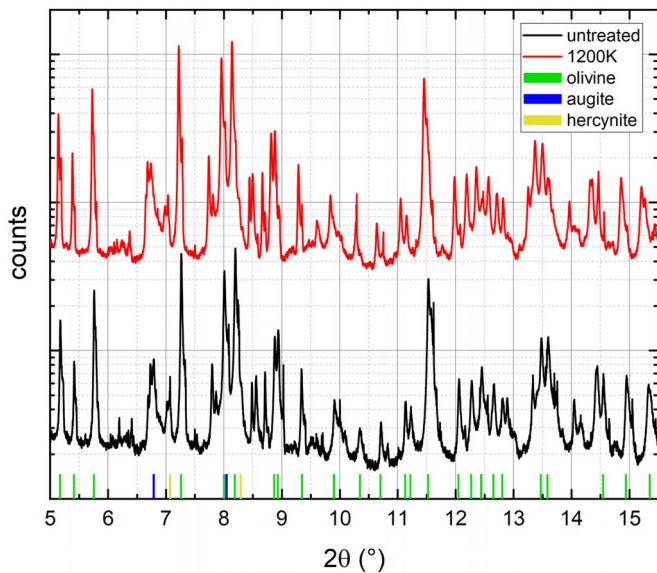

Figure 2. Measured synchrotron X-ray diffractogram of the untreated Allende powder sample (black line), the sample heated up to 1200 K in vacuum (red line), and the most prominent diffraction peaks induced by olivine, augite, and hercynite (colored bars).

Figure 3. Mössbauer spectra of the untreated Allende powder sample measured at 295 K (top) and 5 K (middle), and powder heated at 1200 K in vacuum measured at 295 K (bottom) including all subspectra.

olivines. The remaining peaks are induced by augite (a pyroxene) and hercynite (aluminum spinel, detected in the Allende meteorite by Clarke et al. 1971). The presence of minerals such as pentlandite, reported previously in the Allende meteorite (Bland et al. 2004), could not be verified in our XRD data. Also, no clear signs of goethite could be discerned in the diffractogram, despite it being present in Mössbauer spectra below, which could be explained by partial crystallization of goethite, as previously described by Murad & Schwertmann (1983). The thermal evolution of the diffractograms does not show any significant changes in composition, but only slight shifts (see the data measured at 1200 K in Figure 2), matching the reported thermal expansion coefficients of olivines (Suzuki et al. 1981). As XRD peak shapes and intensities remain widely similar under temperature variation, no significant mineral transformations are to be expected. However, to be more sensitive to compositional changes of iron-bearing minerals, Mössbauer spectroscopy is employed for further analysis.
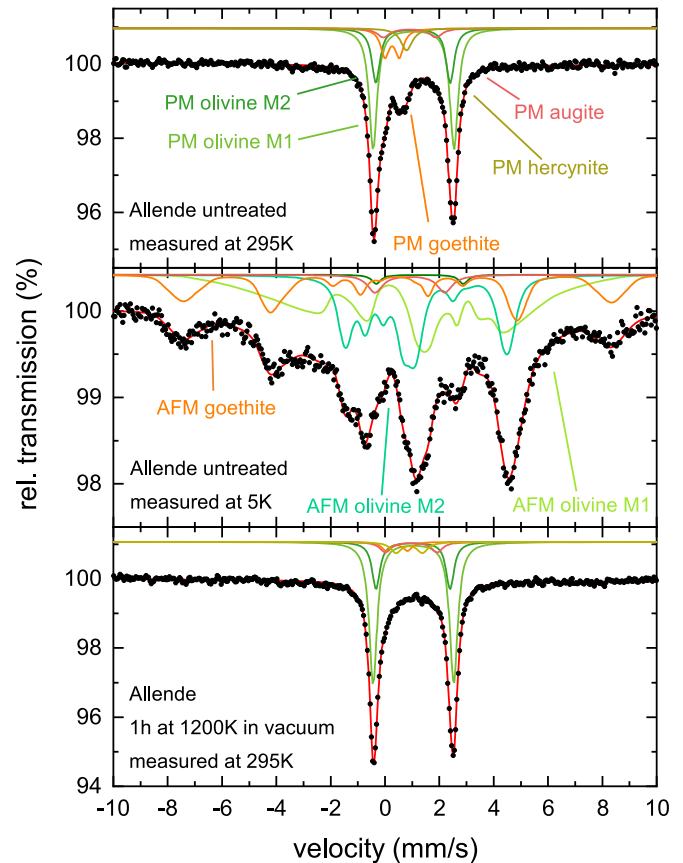
4. Mössbauer Spectroscopy

4.1. Untreated Sample

As Mössbauer spectroscopy is sensitive to the valence state of Fe atoms and the symmetry of their neighboring atoms, it is used to identify Fe-bearing phases in the chondrite. The spectrum of the untreated powder sample of the Allende meteorite measured at room temperature is shown in the top image of Figure 3. It features a distinct doublet structure with two peaks at approximately -0.41 and $2.50\,\mathrm{mm\,s^{-1}}$, respectively, which is induced by olivine. Due to the high amount of olivine in the powder, it is possible to resolve the signals of two

nonequivalent Fe sites M1 and M2 (Sklute 2006). Between the peaks of the olivine doublet, a structure consisting of three independent phase contributions is visible: an augite (pyroxene) doublet, a goethite doublet (α-FeO(OH)), and a hercynite singlet (FeAl$_2$O$_4$), identified based on the characteristic hyperfine parameters as described below. Well-ordered goethite is typically antiferromagnetic up to 400 K, which results in a sextet structure in the Mössbauer spectrum (Murad 1998). A substitution of Fe for Al as well as poor crystallinity can lead to a reduction of the Néel temperature T_N and therefore evoke a paramagnetic doublet structure even at room temperature (Fysh & Clark 1982; Murad & Schwertmann 1983; Berquó et al 2007). Poorly ordered crystals could be a reason for the absence of goethite diffraction peaks in the X-ray diffractograms. Furthermore, isomer shift ($\delta \approx 0.35$ mm s^{-1} relative to $\alpha -$ iron at room temperature) and quadrupole splitting ($\Delta E_Q \approx 0.53$ mm s^{-1}) of the doublet agree well with the hyperfine parameters of those systems.

The middle image of Figure 3 shows the Mössbauer spectrum of the untreated sample measured at 5 K. This temperature falls well below the Néel temperature T_N of goethite, so that it orders antiferromagnetically, resulting in a sextet structure with a distribution of hyperfine fields ($\langle B_{HF} \rangle = 49 \pm 3$ T). The parameters found for this subspectrum are in agreement with those of poorly crystallized goethite (Murad & Schwertmann 1983). As already discussed in Bogdan et al. (2020), antiferromagnetic ordering of olivine leads to the appearance of two octet structures at low temperatures, induced by the M1 and M2 lattice sites. Only a small percentage of olivine remains in the paramagnetic state. Even at 5 K, augite does not order magnetically, and there is still a doublet of similar area compared to the room-temperature measurement detectable. The contribution of hercynite can no longer be resolved at 5 K, due to the superposition with several other more pronounced spectral contributions.

4.2. Heating in Vacuum

The bottom panel in Figure 3 demonstrates the thermal evolution of composition for the vacuum-heated sample set, representatively displaying the room-temperature Mössbauer spectrum of a sample heated at 1200 K. In agreement with XRD data, the olivine doublet remains the dominant spectral contribution, with the hyperfine parameters mostly unchanged under exposure to elevated temperatures. The only significant change induced by heating is the decline in the goethite contribution with every tempering step starting at 1000 K, disappearing completely after exposure to a temperature of 1300 K (top image of Figure 4).

4.3. Heating in Hydrogen Atmosphere

The thermal evolution of the hydrogen-tempered sample shows a similar trend compared to the vacuum-tempered sample up to a temperature of 1000 K (see the top image of Figure 5). As a minor difference, goethite apparently no longer displays a clear doublet structure, but instead a broad sextet distribution with low hyperfine fields, which may indicate a state slightly below the Néel temperature, possibly increased by thermal treatment improving the goethite crystallinity. However, higher temperatures give rise to new contributions in the Mössbauer spectrum, a singlet (blue line) overlapping with the left peak of the olivine doublet and an additional sextet (light
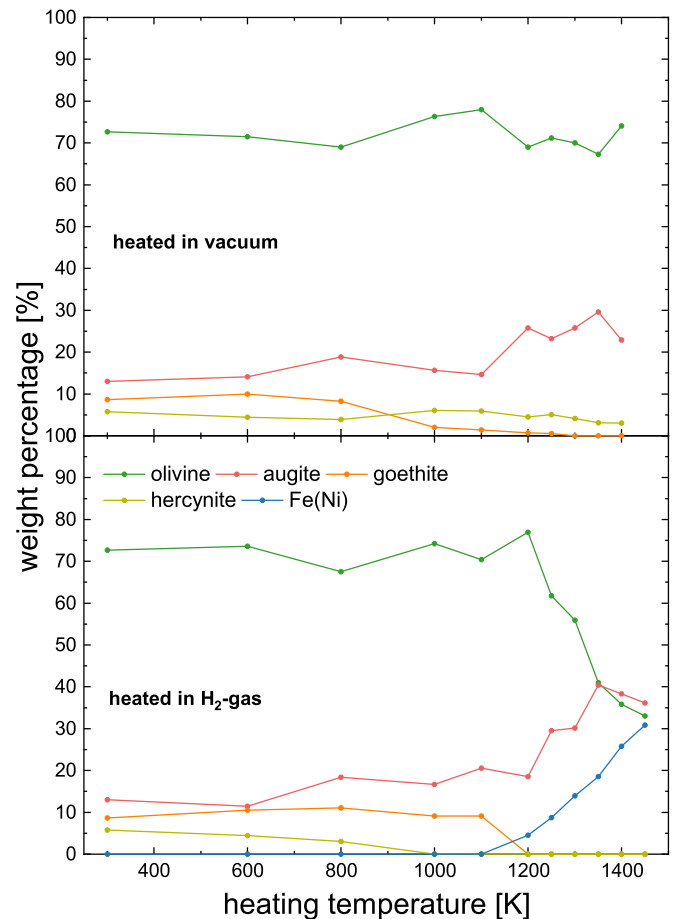

Figure 4. Weight percentages of the identified phases found in the tempered powder samples based on relative spectral areas observed in Mössbauer spectroscopy. The top image shows powder heated in vacuum, while the bottom image shows hydrogen heating.

blue line), as is visible in the bottom image of Figure 5, showing the room-temperature spectrum of the sample after exposure to 1400 K in the hydrogen atmosphere. Based on the characteristic hyperfine parameters, both features can be ascribed to metallic Fe(Ni) phases. The singlet ($\delta = -0.07$ mms^{-1}) is likely induced by taenite, exhibiting an fcc lattice structure, while the sextet displays similar hyperfine parameters ($B_{HF} = 34.5$ T) to kamacite, a bcc Fe(Ni) phase. Combined, they amount to over 50 % of the entire spectral area.

The relative areas of the contributions in the Mössbauer spectra can be roughly converted into weight percentages if the molar fraction of iron in the phases is known (see Figure 4). Based on the lattice parameters extracted from XRD (Cyrus Jahanbagloo 1969) and the observed Néel temperature of approximately 16 K (Belley et al. 2009), an olivine stoichiometry of (Mg$_{0.5}$Fe$_{0.5}$)$_2$SiO$_4$ was assumed. The shape of the pyroxene doublet was compared to a series of Mössbauer spectra of synthetic Mg–Fe pyroxenes (Klima et al. 2007), leading to an estimate of pyroxene stoichiometry of (Mg$_{0.5}$Fe$_{0.5}$)$_2$Si$_2$O$_6$. According to the findings from XRD analysis, the iron content in the silicates is not expected to change considerably by heating in vacuum. For goethite, there was no Al substitution assumed for calculating the weight percentage. The top image of Figure 4 shows the weight distributions of the vacuum-heated powder sample. While there are no significant changes up to around 1000 K, the goethite
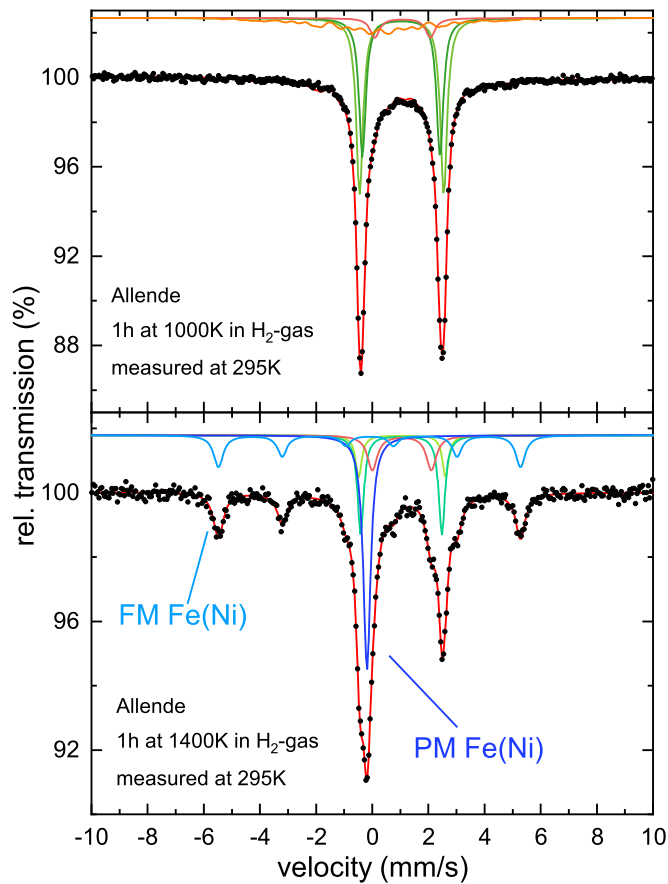
Figure 5. Room-temperature Mössbauer spectra of the Allende powder sample heated at 1000 K (top image) and 1400 K (bottom image) in a hydrogen atmosphere. The contributions induced by Fe(Ni) phases are marked.

Figure 6. The density of solids ρ_{Dust} was estimated based on powder composition extracted from the Mössbauer spectroscopy experiments shown in Figure 4. The distinct increase of ρ_{Dust} starting at 1200 K originates from the reduction of goethite and olivine to metallic Fe(Ni).

contribution vanishes and the pyroxene contribution rises slightly for higher heating temperatures.

The sample tempered in a hydrogen atmosphere (bottom image of Figure 4) shows a similar behavior up to 1000 K. At 1200 K, however, goethite cannot be detected anymore, while the features induced by metallic Fe(Ni) start to arise. A reduction of goethite to a metallic phase can be assumed. Increasing heating temperatures lead to the olivine contribution declining strongly in favor of taenite and pyroxene. This coincides with the known reduction reaction of olivines, breaking down to iron-poorer olivines, metallic Fe(Ni), and pyroxene (Boland & Duba 1981). After heating at 1400 K in H_2 gas, the sample consists of nearly equal amounts of olivine, pyroxene, and Fe(Ni) phases, and the latter might experience enhanced magnetic aggregation (Bogdan et al. 2023).

The powder density can be calculated based on the extracted weight percentages, remaining nearly constant at approximately $3.7 \, g \, cm^{-3}$ for the vacuum-heated powder at all temperatures. The reduction of goethite and olivine to metallic iron leads to a drastic increase in density up to nearly $5 \, g \, cm^{-3}$ (see Figure 6). As in Bogdan et al. (2020) and Pillich et al. (2021), these values were used for the evaluation of the surface energies γ_e of the powder samples.

5. Discussion

The goal of this study was to see if a hydrogen atmosphere has a significant influence on the effective surface energy and what effects minor variations in the initial material composition
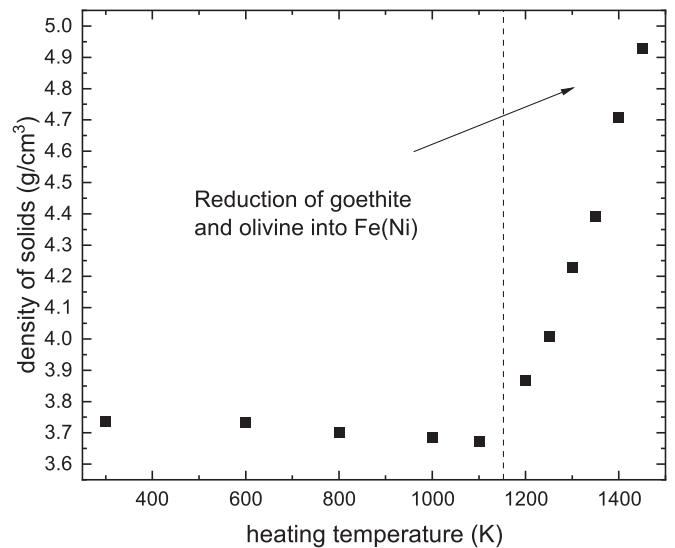
might have. The latter was simulated by the choice of a second meteorite (Allende). The general trend of the surface energy does not change considerably irrespective of material and atmosphere. The surface energy changes within a factor of a few up to 1000 K tempering, but increases by orders of magnitude up to about 1400 K.

As outlined in our earlier work, the interaction of the surfaces getting in contact between two grains matters. These surface forces obviously depend on the composition of the surface. At what depth below the surface specific molecules still matter is not well defined. For a homogeneous body, this would be no issue, but for a heterogeneous body, this might be important. The surface forces are certainly set by the bulk composition of the grains. However, volatiles on the surface can change the interaction strongly. Water is among the most abundant volatiles and hydrophilic surfaces typically have several layers of hydrogen at ambient conditions. The last monolayer is exceptionally well bound. In our earlier studies, we could show that the reduction of the water to one monolayer increases the sticking (surface energy) by a factor of 10 (Bogdan et al. 2020). With any layer of water, the underlying bulk composition still has an influence, though—i.e., the slight compositional changes in silicates upon heating up to about 1000 K changed the surface energy, but only by a factor of a few. Especially iron oxides, though, which were generated in an oxidizing atmosphere earlier, increased the sticking (Pillich et al. 2021). These are not present in the current study. At high temperatures, we consider the removal of the last monolayer of water to set the increasing scale of surface energy.

At the high temperatures, the bulk composition then has to set the surface forces. The hydrogen atmosphere used here has a significant influence at high temperatures beyond 1000 K and produces slightly different results than tempering in vacuum. It essentially generates metallic iron and more augite at the expense of olivine. The stronger surface energy of iron might be visible as the jump in surface energy at about 1100 K. The surface energy for the sample tempered in hydrogen then seems to increase somewhat less steeply than for the sample tempered in vacuum.

There are still some mineral transformations going on, as probed by Mössbauer spectroscopy, but there seems to be no specific mineral that would offset the strong increase due to the metallic iron. This might need some reconsiderations with respect to particle size. The surface morphology might matter here, i.e., how large the contact area between two grains is. As long as the densities of the evolving minerals are comparable, the grains might keep their structure. However, with iron having a much higher density, there has to be a reduction in volume covered by material. This can only go along with shrinking or—as shrinking is not indicated by grain size—surface cracks. In fact, in earlier works, we could see large cracks appearing on somewhat larger grains upon tempering (de Beule et al. 2017). This should generally reduce the effective contact area and will be more efficient if metallic iron is produced. This reduces the contact areas and therefore the sticking forces, and is currently our best guess for the somewhat smaller slope on increasing surface energies measured.

6. Conclusions

The atmosphere that meteorite dust particles are subjected to highly influences compositional changes caused by high temperatures—ranging from significant to almost unnoticed upon tempering. Especially the formation of metallic iron phases might influence the aggregation within a protoplanetary disk's magnetic fields apart from simple adhesion (Kruss & Wurm 2018, 2020; Bogdan et al. 2023).

There are detailed changes in the effective surface energy, depending on the initial composition and the atmospheric conditions. These details of the slightly different initial composition of the two meteorites and the atmosphere during tempering (vacuum or hydrogen) result in variations of a factor of a few beyond 1000 K. They are superimposed on a still larger effect that we attribute to water being removed from the surfaces. In general, surface energies increase by 2 to 3 orders of magnitude from 1000 to 1400 K. This supports the idea that there is a location in the warm inner disk at around 1200 K where aggregation is different, likely producing larger aggregates that might favor planetesimal formation. Within the variations tested, these results seem to be robust, irrespective of the exact parameters.

ORCID iDs

Cynthia Pillich ⓘ https://orcid.org/0000-0002-1699-7998

Tabea Bogdan ⓘ https://orcid.org/0000-0003-3649-931X
Janosch Tasto ⓘ https://orcid.org/0009-0001-1906-3007
Joachim Landers ⓘ https://orcid.org/0000-0002-4506-6383
Gerhard Wurm ⓘ https://orcid.org/0000-0002-7962-4961
Heiko Wende ⓘ https://orcid.org/0000-0001-8395-3541

References

Belley, F., Ferré, E. C., Martín-Hernández, F., et al. 2009, E&PSL, 284, 516
Berquó, T. S., Imbernon, R. A. L., Blot, A., et al. 2007, PCM, 34, 287
Bischoff, D., Kreuzig, C., Haack, D., Gundlach, B., & Blum, J. 2020, MNRAS, 497, 2517
Bland, P. A., Cressey, G., & Menzies, O. N. 2004, M&PS, 39, 3
Blum, J., & Wurm, G. 2008, ARA&A, 46, 21
Bogdan, T., Pillich, C., Landers, J., Wende, H., & Wurm, G. 2020, A&A, 638, A151
Bogdan, T., Pillich, C., Landers, J., Wende, H., & Wurm, G. 2023, A&A, 670, A6
Bogdan, T., Teiser, J., Fischer, N., Kruss, M., & Wurm, G. 2019, Icar, 319, 133
Boland, J. N., & Duba, A. 1981, Natur, 294, 142
Clarke, R. S., Jarosewich, E., Mason, B., et al. 1971, SmCES, 1
Connolly, H. C., & Jones, R. H. 2016, JGRE, 121, 1885
Cyrus Jahanbagloo, I. 1969, AmMin, 54, 246
de Beule, C., Landers, J., Salamon, S., Wende, H., & Wurm, G. 2017, ApJ, 837, 59
Demirci, T., Krause, C., Teiser, J., & Wurm, G. 2019, A&A, 629, A66
Demirci, T., Teiser, J., Steinpilz, T., et al. 2017, ApJ, 846, 48
Dominik, C., & Tielens, A. G. G. M. 1997, ApJ, 480, 647
Fysh, S. A., & Clark, P. E. 1982, PCM, 8, 180
Gärtner, S., Gundlach, B., Headen, T. F., et al. 2017, ApJ, 848, 96
Gundlach, B., Schmidt, K. P., Kreuzig, C., et al. 2018, MNRAS, 479, 1273
Hayashi, C., Nakazawa, K., & Nakagawa, Y. 1985, in Protostars and Planets II, ed. D. C. Black & M. S. Matthews (Tucson, AZ: Univ. Arizona Press), 1100
Johansen, A., Blum, J., Tanaka, H., et al. 2014, in Protostars and Planets VI, ed. H. Beuther (Tucson, AZ: Univ. Arizona Press), 547
Kataoka, A., Tanaka, H., Okuzumi, S., & Wada, K. 2013, A&A, 557, L4
Kimura, H., Wada, K., Senshu, H., & Kobayashi, H. 2015, ApJ, 812, 67
Kley, W., & Lin, D. N. C. 1999, ApJ, 518, 833
Klima, R. L., Pieters, C. M., & Dyar, M. D. 2007, M&PS, 42, 235
Kruss, M., & Wurm, G. 2018, ApJ, 869, 45
Kruss, M., & Wurm, G. 2020, PSJ, 1, 23
Leinhardt, Z. M., & Stewart, S. T. 2012, ApJ, 745, 79
Meisner, T., Wurm, G., & Teiser, J. 2012, A&A, 544, A138
Murad, E. 1998, HyInt, 117, 39
Murad, E., & Schwertmann, U. 1983, ClMin, 18, 301
Musiolik, G., Teiser, J., Jankowski, T., & Wurm, G. 2016, ApJ, 818, 16
Musiolik, G., & Wurm, G. 2019, ApJ, 873, 58
Pillich, C., Bogdan, T., Landers, J., Wurm, G., & Wende, H. 2021, A&A, 106, 1
Pinilla, P., Lenz, C. T., & Stammler, S. M. 2021, A&A, 645, A70
Sklute, E. C. 2006, PhD thesis, Mount Holyoke College
Steinpilz, T., Teiser, J., & Wurm, G. 2019, ApJ, 874, 60
Suzuki, I., Seya, K., Takei, H., & Sumino, Y. 1981, PCM, 7, 60
Weidenschilling, S. J. 1977, MNRAS, 180, 57
Wood, J. A. 2000, SSRv, 92, 87
Yamamoto, T., Kadono, T., & Wada, K. 2014, ApJL, 783, L36
Youdin, A. N., & Goodman, J. 2005, ApJ, 620, 459